International Journal of Innovative
Computing, Information and Control
Volume **7**, Number **11**, November **2011**

 ISSN 1349-4198
pp. 6135–6145

FEED-FORWARD NEURAL NETWORK FOR DIRECT TORQUE CONTROL OF INDUCTION MOTOR

Bambang Purwahyudi[1,2], Heri Suryoatmojo[1], Soebagio[1]
Mochamad Ashari[1] and Takhashi Hiyama[3]

[1]Department of Electrical Engineering
Sepuluh Nopember Institute of Technology (ITS)
Sukolilo, P.O. Box 1/SB, Surabaya-Indonesia 60111
bmb_pur@yahoo.com

[2]Department of Electrical Engineering
Bhayangkara University
Surabaya-Indonesia, Indonesia

[3]Graduate School of Science and Technology
Kumamoto University
39-1, Kurokami 2-chome, Kumamoto 860-8555, Japan

Received June 2010; revised October 2010

Abstract. *PI controllers have been widely used in industrial systems application, because they have a simple structure and offer a satisfactory performance for a wide range operation. However, for varieties of plant parameters and the nonlinear operating condition, fixed gain PI controllers cannot provide the desired control performance. In this paper, advanced PI controller was utilized to control the speed of the induction motor in Direct Torque Control (DTC) for electric propulsion application. The proposed method is developed from conventional PI controller combined with feed-forward neural networks (FFNN). The FFNN is used to tune the gain of PI controller. The effectiveness of the complete proposed control scheme is clarified with a variation of speed reference and load torque applied to the motor. Load torque of induction motor depends on the speed rotation and pitch of propeller. Simulation results show the FFNN tuning technique provides better speed control performance.*
Keywords: PI controller, Direct torque control, Neural network, Electric propulsion

1. **Introduction.** Recently, there are many applications of electrical energy used for transportation system especially in marine transportation system. One of them is electric propulsion system. In this system, electric motor is used as prime mover to produce the ship propulsion. The induction motor is the most commonly used in the propulsion system to convert an electrical power to mechanical power because it can be directly connected to the electric network. In the propulsion system, induction motor is directly coupled with propeller of the ship [1-4]. In addition, induction motor has many advantages such as simply in construction, reliable, flexible, inexpensive, high efficiency, fast response and free maintenance [5]. However, induction motor is difficult to maintain a constant speed whenever the load is changed. Actually, there are several methods to solve such kind of problems. Field oriented control (FOC) or vector control method is one of the popular methods to solve the problem. FOC is a field regulation method of AC motor by changing coupled system to decoupled system. By this method, the excitation current and load current can be controlled separately. Hence, flux and torque also can be separately controlled similar in DC motor [5-7].

The FOC method required current controller, coordinate transformation and current regulator to control pulse-width-modulation in the inverter system. They make the FOC method become the complexity [5-7]. Recently, the new control technique well known as Direct Torque Control (DTC) was introduced with different method to control the induction motor torque and flux [4-14]. In DTC methods, the torque and flux are directly controlled by using a voltage vector of the inverter. To determine the voltage vector of the inverter depends on the condition of stator flux hysteresis controller, torque hysteresis controller and sector position of the stator flux.

In the real application, variable speed drive of the induction motor is equipped with a speed controller. Many speed controllers have been used for control of induction motor such as conventional PI, sliding mode controller, etc. [12]. Most popular of the speed controller uses conventional PI controller because of their simple structures and offers a satisfactory performance for wide range operation. However, conventional PI controller equipped with fixed gain only cannot provide the desired control performance if plant parameter is changed or due the nonlinear operation [13-16]. Here, the nonlinearities or changing parameters are occurred whenever a variable speed drive system is fed by an induction motor. Usually, conventional PI controllers use off-line tuning algorithm even if it is very difficult to use in the continuous changing condition [14-17]. Therefore, on-line tuning algorithms are required to provide good performance in variable speed drives [15,16].

Many strategies have been proposed by many researchers to tune the PI controller parameters. The most popular method frequently used in industrial application is the Ziegler-Nichols method. In this method, a system model and the control parameters are required to determine the parameters of the PI controller from the plant step response. However, the step response yields a high overshoot. In addition, the control signal required for the adequate performance of the system is too high. The other technique is frequency response method based on specified phase and gain margins as well as crossover frequency. They are used to improve the performance of the system. In addition, root locus and pole assignment design techniques are proposed to transient response specifications. All these methods are considered as model based strategies and then the efficiency of the tuning law depends on the accuracy of the proposed model and also the assumed conditions with respect to actual operating conditions [13-18].

From the descriptions above, the drawback of the PI controller encourages to develop the conventional PI controller with artificial intelligence (AI) techniques [13-22]. For that reason, utilization of feed-forward neural network (FFNN) in this case attracts the attention of many researchers. The advantage of FFNN is easy in training and generalization, simple architecture [18,25]. In this paper, the gains of the PI controller in DTC of induction motor will be tuned by an adaptive mechanism based on FFNN. By this approach, FFNN can approximate dynamic input output mapping of linear and nonlinear system. To examine the robustness of this method, the induction motor is used for electric propulsion system of the ship because of their complexity for the torque and speed. Load torque of electric propulsion system depends on speed of propeller and also speed of induction motor depends on torque output of propeller. This paper is organized as follows: the mathematical model of induction motor and the basic concept of direct torque control for induction motor drives are described in Section 2; Section 3 shows the load torque model for electric propulsion using propeller; Section 4 shows the development of the FFNN tuning of PI controller parameters based on changing speed of induction motor and load torque of electric ship; the effectiveness of the complete proposed control scheme is clarified through a MATLAB/SIMULINK simulation which is presented in Section 5; the conclusions and references list end this paper.

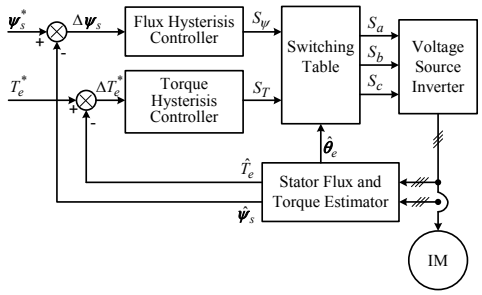

FIGURE 1. Block diagram of DTC

2. **Induction Motor Operation Using DTC.** The dynamic model of the induction motor is derived by transforming the three phase quantities into two phase direct and quadrature axes quantities. The mathematical model can be described in the stationary reference frame as follows:

$$\frac{d}{dt}\begin{bmatrix} i_s \\ \psi_r \end{bmatrix} = \begin{bmatrix} A_{11} & A_{12} \\ A_{21} & A_{22} \end{bmatrix}\begin{bmatrix} i_r \\ \psi_r \end{bmatrix} + \begin{bmatrix} B_1 \\ 0 \end{bmatrix} v_s \tag{1}$$

where,

$$i_s = \begin{bmatrix} i_{sd} & i_{sq} \end{bmatrix}^T \tag{2}$$

$$\psi_r = \begin{bmatrix} \psi_{rd} & \psi_{rq} \end{bmatrix}^T \tag{3}$$

$$v_s = \begin{bmatrix} v_{sd} & v_q \end{bmatrix}^T \tag{4}$$

$$A_{11} = -\left\{ \frac{R_s}{(\sigma L_s)} + \frac{1-\sigma}{\sigma \tau_r} \right\} I \tag{5}$$

$$A_{12} = \frac{M}{(\tau L_s L_r)} \times \left(\frac{1}{\tau_r} I - \omega_r I \right) = \left(\frac{M}{\tau_r} \right) I \tag{6}$$

$$A_{22} = -\left(\frac{1}{\tau_r} \right) I + \omega_r J \tag{7}$$

$$B_1 = \frac{1}{\tau L_s} I \tag{8}$$

$$I = \begin{bmatrix} 1 & 0 \\ 0 & 1 \end{bmatrix} \tag{9}$$

$$J = \begin{bmatrix} 0 & -1 \\ 1 & 0 \end{bmatrix} \tag{10}$$

$$\sigma = 1 - \frac{M^2}{L_s L_r} \tag{11}$$

$$\tau_r = \frac{L_r}{L_r R_r} \tag{12}$$

With, ω_r, i_s, ψ_r, v_s, R_s, R_r, L_s, L_r, M, σ and τ_r are rotor speed, stator current and voltage, stator and rotor resistance, stator, rotor and mutual inductance, linkage coefficient and rotor time constant, respectively.

Rotor speed as function of electromagnetic torque (T_e) and load torque (T_L) can be expressed as:

$$\frac{J}{p}\frac{d\omega_r}{dt} = T_e - T_L - f\omega_r \tag{13}$$

where, J, p and f are inertia moment, number of poles and friction constant, respectively.

Electromagnetic torque (Te) can be obtained from machine flux linkages and current as:

$$T_e = \frac{3}{2}\frac{p}{2}\left(\psi_{sd} i_{sq} - \psi_{sq} i_{sd}\right) \tag{14}$$

Electromagnetic torque can also be expressed in the stationary reference frame as:

$$T_e = \frac{3}{2}\frac{p}{2}\frac{M}{(\sigma L_r L_s)}\left|\psi_r\right|\left|\psi_s\right|\sin\theta_e \tag{15}$$

where, θ_e is the angle between the stator and rotor flux linkage.

2.1. **DTC method strategy.** The block diagram of proposed speed control of induction motor based on DTC method is presented in Figure 1. The DTC method was introduced by Takahashi and Noguchi [5]. This control strategy is relatively new and competitive if it is compared with the rotor flux oriented method. The DTC of induction motor drive is based on the directly command sequence determination applied to the switching of voltage source inverter fed induction motor. The command stator flux and torque magnitude are compared with the respective estimated value. Resulted errors of T_e and s respectively are processed in hysteresis controller. Two output hysteresis controllers and stator flux position in space vector are used to determine one of eight switching combinations in voltage source inverter, two zero voltage vectors and six voltage vectors shown in Figure 2. This determination is used to maintain torque and flux error inside the hysteresis band. The principle operation of DTC can also be described from Equation (15). It is clear described that the electromagnetic torque can be changed by arranging the stator and rotor flux vectors, and their relative position. The rotor flux linkage changes slowly if it is compared to the stator flux linkage because the rotor time constant of induction motor is very large. During a short transient, the rotor flux almost unchanged. Thus rapid changes of electromagnetic torque can be produced by rotating the stator flux in the required direction, which is determined by the torque command.

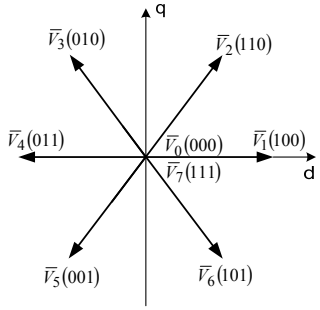

FIGURE 2. Inverter output voltage vectors

The stator flux can be obtained from Equation (16) and if the stator resistance is neglected, the stator flux can be expressed in Equation (17).

$$\bar{\psi}_s = \int_0^t \left(\bar{V}_s - R_s I_s\right) dt \tag{16}$$

$$\bar{\psi}_s = \int_0^t \left(\bar{V}_s\right) dt \tag{17}$$

The voltage vector applied is still constant during one period of sampling T_s. The stator flux of induction motor can be expressed as:

$$\bar{\psi}_s(k) = \bar{\psi}_s(k-1) + \bar{V}_s T_s \tag{18}$$

TABLE 1. Logic control of flux and torque hysteresis controller

Conditions of Flux	**S**
$\mid \psi_s \mid \leq \mid \psi_s* \mid - \mid \Delta\psi_s \mid$	1
$\mid \psi_s \mid \geq \mid \psi_s* \mid + \mid \Delta\psi_s \mid$	0
Conditions of Torque	**ST**
$\mid T_e \mid \leq \mid T_e^* \mid - \mid T_e \mid$	1
$\mid T_e \mid = \mid T_e^* \mid$	0
$\mid T_e \mid \geq \mid T_e^* \mid + \mid \delta T_e \mid$	-1

or

$$\Delta\bar{\psi}_s = \bar{V}_s T_s \tag{19}$$

Equation (19) shows that the stator flux can be increased or decreased by applying suitable stator voltage vector. Stator flux error consists of the radial and the tangential of components shown in Figure 3. The radial component ψ_{st} states the torque action and tangential component ψ_{sf} states the flux action. If the position of stator flux is known, controlling both flux and torque can be done by selecting the suitable inverter voltage vectors. The inverter voltage vectors which are applied to the induction motor are selected

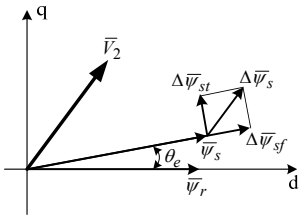

FIGURE 3. Components of the flux error when applying the voltage vector V_2

by using DTC algorithms based on the torque and flux hysteresis controller status and stator flux position sector which is denoted by S_i $(i = 1, 2, \ldots, 6)$. The outputs of the switching table of inverter state the switching combination of switch device of inverter. Table 1 and Table 2 show the logic control of the flux and torque hysteresis controller and switching table of voltage inverter, respectively. Figure 4 shows the relation of inverter voltage vectors and the stator flux position sectors. The dividing of six stator flux sectors as follows: $-30° < S_1 < 30°$, $30° S_2 < 90°$, $90° S_3 < 150°$, $150° S_4 < 210°$, $210° S_5 < 270°$ and $270° < S_6 < 330°$, respectively.

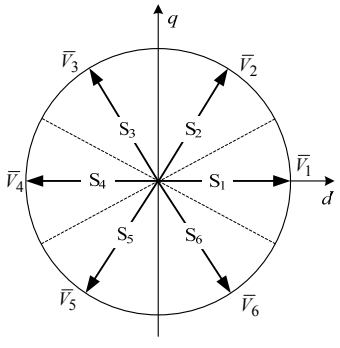

FIGURE 4. Inverter voltage vectors and stator flux sectors

TABLE 2. Switching table of inverter voltage

S_ψ	S_T	Stator Flux Sectors					
		S_1	S_2	S_3	S_4	S_5	S_6
1	1	V_2	V_3	V_4	V_5	V_6	V_1
1	0	V_7	V_0	V_7	V_0	V_7	V_0
1	–1	V_6	V_1	V_2	V_3	V_4	V_5
0	1	V_3	V_4	V_5	V_6	V_1	V_2
0	0	V_0	V_7	V_0	V_7	V_0	V_7
0	–1	V_5	V_6	V_1	V_2	V_3	V_4

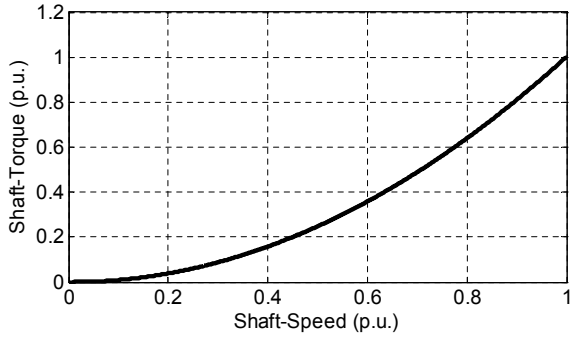

FIGURE 5. Speed-torque characteristic of full pitch propeller

3. **Load Torque Model of Electric Propulsion.** Load torque in electric propulsion system has a specific characteristic. The electric power provided by the power plant is used to propel the ship. It must be used to rotate a shaft connected between induction motor and the propeller. The rotation force is necessary to turn the shaft is simply torque [1-3]. The torque obtained by the propeller is based on its speed rotation and pitch angle. Typically for induction motor, power and available torque are provided as curves on performance data sheets as a plot of torque as a function of shaft rotation speed. Figure 5 shows the load characteristics for an induction motor with load curves for a full pitch propeller [1-3,26].

4. **Proposed Speed Controller Strategy.**

4.1. **Model system.** The block diagram of model system proposed is shown in Figure 6. The conventional speed controller still use fixed PI controller to control the rotor speed of induction motor, however for the variation plant parameter and operating condition, it do not provide the satisfying control performance. In this paper, gain of PI controllers (K_p, K_i) must be changed to follow the variation plant parameter and operating condition. The propose method is feed-forward neural network (FFNN). FFNN is used to tune the gain of PI controller, so that will obtain the satisfying control performance.

4.2. **Gain tuning of PI speed controller using FFNN.** FFNN is a machine like human brain with properties of learning capability and generalization. They require a lot of training to understand the model of the plant. The basic property of this network is capably to approximate complicated nonlinear functions. The FFNN uses a dense interconnection of neurons that correspond to computing nodes. Each node performs the multiplication of its input signals by constant weights, sums up the results, and maps the sum to a nonlinear function; the result is then transferred to its output. The FFNN consists of three layers, an input layer, one or more hidden layers, and an output

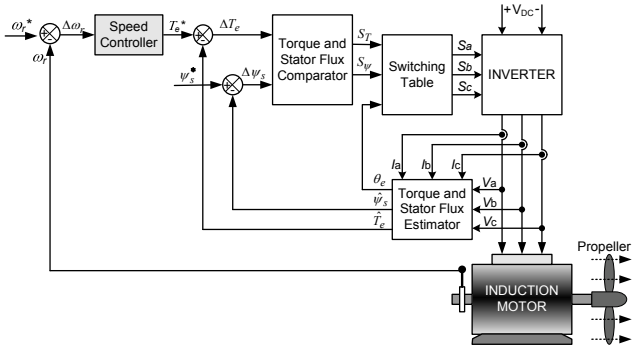

FIGURE 6. Block diagram of model system

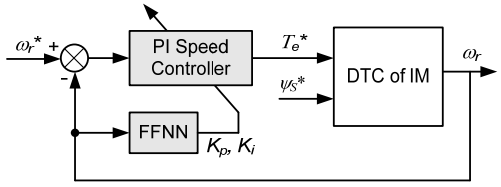

FIGURE 7. Tuning PI controller using FFNN

layer. Hidden and output neurons generally have an activation function. The knowledge of FFNN is acquired through a learning algorithm, which performs the adaptation of weights of the network until the error between the target vectors and output of network according to a desired error. The most popular learning algorithm for FFNN is the back propagation algorithm, which consists of a forward and backward action. In the forward action, the signals are processed through the network layer by layer. The output vector is generated and subtracted from the desired output vector. The resultant error vector is propagated backward in the network and serves to adjust the weights in order to achieve the desired output error [11,18,21,23].

In this paper, FFNN is used to tune the gain PI controller (K_p and K_i). The block diagram of tuning PI controller using FFNN is shown in Figure 7. The proposed FFNN consists of an input layer, a hidden layer and an output layer. The input layer has a neuron representing rotor speed of induction motor. The hidden layer has ten neurons. The output layer is composed of two neurons, each representing the gain proportional (K_p) and the gain integral (K_i) controller. The activation function of the hidden layer is hyperbolic tangent sigmoid function and the activation function of the output layer is linear transfer function. The data training of FFNN is taken from the optimum value of gain PI controller for each conditions of rotor speed of induction motor. The learning of the FFNN is done using the Levenberg-Marquardt back-propagation algorithm with a number of epochs 1000 and a goal error of 10^{-3}. Table 3 shows the data training for FFNN.

5. **Simulation Result.** The effectiveness of the complete proposed control scheme is clarified with a variation of speed reference and load torque applied to the motor and compared with conventional fixed PI speed controller using MATLAB/SIMULINK. A simple block diagram for simulation of model system is shown in Figure 8. Load torque applied in this system using electric propulsion system which depends on rotation speed and pitch angle of propeller. The nominal operating condition and system parameters are given in Appendix. The FFNN is applied to the gain PI speed controller tuning called

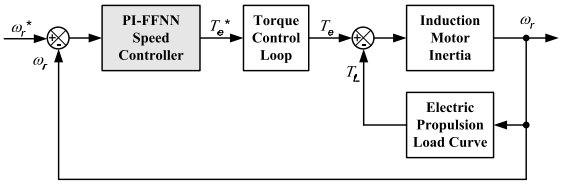

FIGURE 8. Simple block diagram for simulation

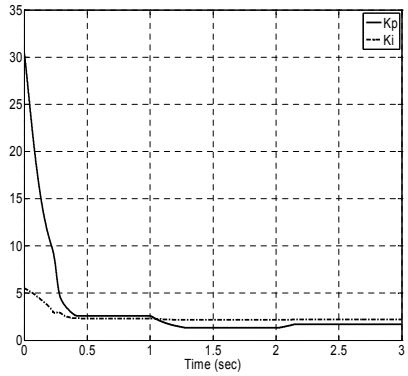

FIGURE 9. Various gain of PI controllers

PI-FNN controller. Load torque of induction motor is taken from load characteristic of full pitch propeller as shown in Figure 5. The simulation of proposed strategy method is done in three operating condition for starting, accelerating and decelerating. The starting condition is begun at 0 s and speed of induction motor gradually change from 0 to 60 rad/s. The accelerating condition is started at 1 s and speed of induction motor is gradually changed from 60 to 100 rad/s. A last operating condition is decelerating condition which begun at 2 s and speed of induction motor is gradually decreased from 100 to 80 rad/s. The change of speed of induction motor also cause the change of load torques for each operating conditions from 0 to 1.57 N.m, from 1.57 to 4.37 N.m and from 4.37 to 2.80 N.m.

5.1. **Comparison of gain of PI controller.** Figure 9 shows the variation of proportional gain (K_p) and integral gain (K_i) for PI-FFNN controller. K_p and K_i for fixed PI controller are 2.5 and 2.3 respectively. Simulation result show that the gains of PI-FNN controllers always changes if the rotors speed of induction motor is changed during control operation. However, the gain of fixed PI controller will not change even though the rotor speed of induction motor is changed.

5.2. **Comparison of rotor speed response.** Comparison of steady state error for rotor speed of induction motor by using fixed PI controller and PI-FFNN controller are shown in Table 4. Rotor speed of induction motor are gradually changed 60, 100 and 80 rad/sec. Variation of speed reference describe starting, accelerating and decelerating condition of systems. Table 4 shows that steady state error of fixed PI controller and PI-FFNN controller are 0.5 rad/sec and 0.1 rad/sec when rotor speed of induction motor is gradually operated from 0 to 60 rad/sec. Steady state error of fixed PI controller and PI-FFNN controller are 1.1 rad/sec and 0.6 rad/sec when rotor speed of induction motor is gradually operated from 60 to 100 rad/sec. Steady state error of fixed PI controller and PI-FFNN controller are 0.2 rad/sec and 0.1 rad/sec when rotor speed of induction motor is gradually

TABLE 3. Data trainning

Speed	10	20	30	40	50	60	70	80	90	100	110	120	130	140
K_p	21.71	14.57	9.75	5.35	3.38	2.62	2.08	1.74	1.49	1.31	1.17	1.05	0.96	0.86
K_i	1.14	1.12	1.11	1.1	1.1	1.09	1.08	1.07	1.07	1.06	1.04	0.97	0.83	0.67

TABLE 4. Error steady state (rad/sec)

Rotor speed (rad/sec)	PI	PI-FFNN
60	0.5	0.1
100	1.1	0.6
80	0.2	0.1

TABLE 5. Electromagnetic torque of induction motor (N.m)

Rotor speed (rad/sec)	PI	PI-FFNN
0-60	5.54	5.32
60	1.57	1.57
60-100	8.12	7.79
100	4.37	4.37
100-80	–0.99	–1.04
80	2.8	2.8

TABLE 6. Stator current (A)

Rotor speed (rad/sec)	PI	PI-FFNN
0-60	3.13	3.09
60	2.76	2.76
60-100	3.56	3.53
100	3.02	3.02
100-80	2.69	2.65
80	2.84	2.84

operated from 100 to 80 rad/sec. Therefore, PI-FFNN controller is better than fixed PI controller.

5.3. **Comparison of torque response.** Comparison of electromagnetic torque for the fixed PI controller and PI-FFNN controller are shown in Table 5. Induction motor is operated at variation of speeds and load torques (T_L). The changes of T_L in electric propulsion system depend on rotor speed of induction motor directly connected propeller. The T_L applied induction motor according to speed-torque characteristic of full pitch propeller in Figure 5. Change of electromagnetic torque T_e will basically follow the variation of T_L. Table 5 shows that, T_e is greater than the load torque (T_L) when rotor speed is gradually accelerated from 0 to 60 rad/sec. Difference between T_e and T_L is used to accelerate the speed of induction motor. Otherwise, the T_e is smaller than the load torque (T_L) when rotor speed is gradually decelerated from 100 to 80 rad/sec. The T_e is equal T_L when rotor speed of induction motor are 60, 80 and 100 rad/sec. Therefore, PI-FFNN controller require T_e small than fixed PI controller.

5.4. **Comparison of stator current response.** Comparison of stator current for the fixed PI controller and PI-FFNN controller are shown in Table 6. Simulation results show

that value of stator current will changes when the Te changes. Value of stator current will increase when electromagnetic torque increase. Table 6 shows that stator currents are respectively 2.76, 3.02 and 2.84 A when rotor speeds of induction motor are 60, 100 and 80 rad/sec if the system use fixed PI controller. And also, stator current are 3.13, 3.56 and 2.69 A when rotor speed of induction motor are respectively change from 0 to 60, from 60 to 100 and from 100 to 80 rad/sec. At the same condition of simulation, if the system use PI-FFNN controller, stator currents are respectively 2.76, 3.02 and 2.84 A when rotor speed of induction motor are 60, 100 and 80 rad/sec. And also, stators current are 3.09, 3.53 and 2.65 A when rotor speeds of induction motor are change from 0 to 60, from 60 to 100 and from 100 to 80 rad/sec. Therefore, PI-FFNN controller require stator current small than fixed PI controller.

6. **Conclusion.** Gain tuning of PI speed controller based on feed-forward neural network (FFNN) has been presented. FFNN was utilized to tune the gain of PI speed controller. Meanwhile, training data used in this model were taken from the optimum value of gain PI controller for each rotor speed and load torque conditions. Load torque of the induction motor applied in the electric propulsion system were depending on the rotor speed of the induction motor directly connected the propeller. The simulation results show that the rotor speed of induction motor for PI-FFNN controller method provides small steady state error compared with fixed PI controller. The electromagnetic torque yielded both these methods is greater than the load torque when the rotor speed of the induction motor was accelerated from 0 to 60 rad/sec and from 60 to 100 rad/sec. Otherwise, the electromagnetic torque yielded both these methods was smaller than the load torque when rotor speed of the induction motor was decelerated from 100 to 80 rad/sec. The electromagnetic torque used to accelerate and decelerate the speed of the induction motor by using PI-FFNN controller was smaller than with using fixed PI controller. The magnitude of the stator current will be changed, if the electromagnetic torque of the induction motor speed was changed. The magnitude of the stator current of the induction motor using PI-FFNN controller was also smaller than with using fixed PI controller.

REFERENCES

[1] A. K. Adnanes, Maritime electrical installations and diesel electric propulsion, *ABB AS Marine*, Oslo, 2003.

[2] A. H. Techet, *Hydrodynamics for Ocean Engineers, Course Material of Hydrodynamic*, Massachusetts Institute of Technology, 2004.

[3] *http://www.industry.siemens.com/marine/en/solution/siship.htm.*

[4] J. Faiz, S. H. Hossieni, M. Ghaneei, A. Keyhani and A. Proca, Direct torque control of induction motor for electric propulsion systems, *Electric Power Systems Research*, vol.51, pp.95-101, 1999.

[5] G. Buja and M. P. Kazmierkowski, Direct torque control of PWM inverter-fed AC motors – A survey, *IEEE Transactions on Industrial Electronics*, vol.51, no.4, pp.744-757, 2004.

[6] X. D. T. Garcia, A. Arias, M. G. Taine, P. A. Witting, V. M. Sala and J. L. Romeral, New DTC control scheme for induction motors fed with a three-level inverter, *AUTOMATIKA*, vol.46, no.1-2, pp.73-81, 2005.

[7] A. Abbou and H. Mahmoudi, Performance of a sensorless speed control for induction motor using DTFC strategy and intelligence technique, *Journal of Electrical Systems*, vol.5, no.3, 2009.

[8] I. Takahashi and T. Noguchi, A new quick-response and high-efficiency control strategy of and induction motor, *IEEE Transactions on Industrial Applications*, vol.IA-22, no.5, pp.820-827, 1986.

[9] M. Depenbrock, Direct self control of inverter-feed induction machines, *IEEE Transactions in Power Electronics*, vol.3, no.4, pp.420-429, 1988.

[10] B. Purwahyudi and M. Ashari, Usage radial basis function (RBF) voltage vector direct torque control (DTC) PWM inverter, *Proc. of Seminar Nasional Teknologi Informasi dan Aplikasinya*, Malang, Indonesia, 2009.

[11] R. Kumar, R. A. Gupta, S. V. Bhangale and H. Gothwal, Artificial neural network based direct torque control of induction motor, *IETECH Journal of Electrical Analysis*, vol.2, no.3, pp.159-165, 2008.
[12] C.-Y. Chen, Sliding mode controller design of induction motor based on space-vector pulse width modulation method, *International Journal of Innovative Computing, Information and Control*, vol.5, no.10(B), pp.3603-3614, 2009.
[13] S. M. Gadoue, D. Giaouris and J. W. Finch, Tuning of PI speed controller in DTC of induction motor based on genetic algorithms and fuzzy logic scheme, *Proc. of the 5th International Conference of Technology and Automation*, Thessaloniki, Greece, pp.85-90, 2005.
[14] S. M. Gadoue, D. Giaouris and J. W. Finch, Artificial intelligence-based speed control of DTC induction motor drives – A comparative study, *Electric Power System Research*, vol.79, pp.210-219, 2009.
[15] M. N. Uddin, T. S. Radwan and M. Rahman, Performance of fuzzy-logic-based indirect vector control for induction motor drive, *IEEE Transactions on Industrial Applications*, vol.38, no.5, pp.1219-1225, 2002.
[16] M. Nour, O. Bouketir and C. E. Yong, Self tuning of PI speed controller gains using fuzzy logic controller, *Modern Applied Science*, vol.2, no.6, pp.55-65, 2008.
[17] F. Lin, H. Shieh, K. Shyu and P. Huang, Online gain tuning IP controller using real-coded genetic algorithm, *Electric Power System Research*, vol.72, pp.157-169, 2004.
[18] K. C. Chan and S. S. Leong, A neural network PI controller tuner, *Artificial Intelligence in Engineering*, vol.9, pp.167-176, 1995.
[19] Z. Y. Zhao, M. Tomizuka and S. Isaka, Fuzzy gain scheduling of PID controllers, *IEEE Trans. on Systems, Man, and Cybernetics*, vol.23, no.5, 1993.
[20] L. Mokrani and K. Kouzi, Influence of fuzzy adapted scaling factors on the performance of a fuzzy logic controller based on an indirect vector control for induction motor drives, *Journal of Electrical Engineering*, vol.55, no.7-8, pp.188-194, 2004.
[21] M. A. Denai and S. A. Attia, Fuzzy and neural control of an induction motor, *International Journal Applications on Mathematical and Computer Science*, vol.12, no.2, pp.221-233, 2002.
[22] T. J. Ren and T. C. Chen, Robust speed-controlled induction motor drive based on recurrent neural network, *Electric Power System Research*, vol.76, pp.1064-1074, 2006.
[23] M. Wlas, Z. Krzeminski and H. A. Toliyat, Artificial-neural network based sensorless nonlinear control of induction motor, *IEEE Transactions on Energy Conversion*, vol.20, no.3, 2005.
[24] A. K. Muhamad and T. Hiyama, Induction motor bearing failure diagnosis with ANN and hybrid networks model, *ICIC Express Letters*, vol.3, no.3(B), pp.543-548, 2009.
[25] J. Yi and Y. Li, A RBF neural network based optimization model and its application in mechanical manufacturing production plan, *ICIC Express Letters*, vol.4, no.3(B), pp.1033-1038, 2010.
[26] *http://www.kamome-propeller.co.jp/en/brochures/pdf/kamome_smart_way_ccp_eng.pdf.*

Appendix. The induction motor parameters applied for simulation are as follows: rated voltage of 380 V, 4 poles, 50 Hz, nominal rotor speed of 150.8 rad/s, nominal stator flux of 1.74 Wb, stator resistance of 1.7, rotor resistance of 1.34, stator inductance of 459.2 mH, rotor inductance of 457 mH, mutual inductance of 442.5 mH inertia moment of 0.025 Kg.m^2, and friction coefficient of 1e-5 Kg.m^2/s.